IJASRaR
ISSN: 3062-2751

**International Journal of Applied Sciences and Radiation Research**

*Vol. 3-No.1 (2026) pp. 54-58* https://doi.org/10.22399/ijasrar.67

**Research Article** *www.ijasrar.com*

# Radiation Shielding of Glasses in terms of Exposure Build-up Factors

**M. Shaheer Akhtar[1]*, Nuray Kutu[2], Işık Yeşim Erdamar[3], Seher Polat[4], Eren Urtekin[5]**

[1]New & Renewable Energy Material Development Center (New REC), Jeonbuk National University, Republic of Korea

* **Corresponding Author Email:** shaheerakhtar@jbnu.ac.kr - **ORCID:** 0000-0002-5247-1150

[2]Süleyman Demirel Üniversity, Isparta-Turkiye
**Email:** nuray.kutu@sdu.edu.tr-**ORCID:** 0000-0002-1147-9950

[3]Dicle University, Faculty of Education, Diyarbakır, Türkiye
**Email:** ydicle@dicle.edu.tr - **ORCID:** 0000-0001-8085-0926

[4]Sakarya Üniversity, Sakarya-Turkiye
**Email:** aseher@sakarya.edu.tr- **ORCID:** 0000-0002-5227-0050

[5]Avrasya University, Trabzon, Türkiye
**Email:** erenurtekin@avrasya.edu.tr- **ORCID:** 0000-0002-5207-1850

**Article History:**

**DOI:** 10.22399/ijasrar.67
**Received:** Aug. 03, 2026
**Revised:** Sep. 27, 2026
**Accepted:** Sep. 28, 2026

**Keywords:**

Exposure build-up factor;
Barium titanophosphate glass;
Gamma-ray shielding;
Geometric-progression method;
Phy-X/PSD

**Abstract:** Exposure build-up factor (EBF) is an important quantity for estimating the contribution of scattered photons to exposure behind a shielding material. In this study, the energy-dependent EBFs of four barium titanophosphate glasses with nominal compositions $20Ba–(5+x)TiO_2–(75−x)P_2O_5$ (x = 0, 5, 10 and 15 mol%) were evaluated computationally. The glass densities range from 2.93 to 3.33 g $cm^{-3}$. EBF values were obtained using the Phy-X/PSD platform and the geometric-progression fitting method with ANSI/ANS-6.4.3 reference coefficients. The calculations cover 25 photon energies and penetration depths from 0.5 to 40 mean free paths (mfp). The EBF curves are close to unity at low photon energies, increase to broad maxima in the 0.4–0.8 MeV region, and decrease at higher energies. The maximum EBF increases markedly with penetration depth; for TiO-1, values of 1.85, 6.18, 13.8 and 35.4 are obtained at 1, 5, 10 and 20 mfp, respectively. Between 0.1 and 3 MeV, the $TiO_2$-rich composition exhibits EBF values up to approximately 8% lower than the $TiO_2$-poor composition. These findings show that photon energy, penetration depth and glass composition influence the scattered-photon contribution and should be considered when assessing these glasses for gamma-ray shielding.

## 1. Introduction

Ionising radiation is routinely used in medical diagnosis and therapy, nuclear energy production, industrial radiography and scientific research. Shielding design must therefore account not only for primary photons but also for photons scattered within the shielding material. In broad-beam conditions, scattered photons can contribute substantially to the exposure at a point behind the shield. The exposure build-up factor (EBF), defined as the ratio of the total exposure including scattered photons to the exposure due to uncollided photons, is consequently an important parameter in practical shielding calculations [1,2].Oxide glasses are of interest as radiation-shielding materials because they combine optical transparency with compositional flexibility. Their density and elemental composition can be adjusted by changing the glass-forming and modifying oxides. Phosphate glasses are particularly attractive because $P_2O_5$ supports relatively low melting temperatures and accommodates a range of metal cations. However, simple phosphate glasses may exhibit limited chemical durability. Incorporating $TiO_2$ can improve network connectivity and chemical durability through the formation of P–O–Ti linkages, while also changing the density and local composition of the glass [3–7].
Barium-containing phosphate and titanophosphate glasses have been investigated for optical and shielding-related applications. Previous work has reported the formation and structural properties of

$BaO–TiO_2–P_2O_5$ glasses and has shown that $TiO_2$ content affects their density and molar volume [8]. Nevertheless, the EBF response of this glass series has not been specifically examined. Since EBF depends on photon energy, penetration depth and the effective atomic number of the material, a focused assessment is needed to understand the role of $TiO_2$ substitution in the contribution of scattered photons.

Accordingly, this study examines only the exposure build-up factor of four $Ba–TiO_2–P_2O_5$ glass compositions. Other photon attenuation parameters, neutron interaction quantities and energy-absorption build-up factors are outside the scope of the revised manuscript.

## 2. Materials and methods

### 2.1. Glass compositions

Four glass compositions in the series $20Ba–(5+x)TiO_2–(75−x)P_2O_5$ (x = 0, 5, 10 and 15 mol%) were considered and labelled TiO-1 to TiO-4. The densities used in the calculations were 2.93, 3.04, 3.18 and 3.33 g $cm^{-3}$, respectively. The nominal compositions and densities are presented in Table 1. Elemental mass fractions were derived from the nominal formula and standard atomic masses.

***Table 1.*** *Nominal compositions and densities of the investigated glasses.*

| Code | Nominal composition (mol%) | Density, ρ (g $cm^{-3}$) | $TiO_2$ content (mol%) |
|---|---|---|---|
| S1 | $20Ba–5TiO_2–75P_2O_5$ | 2.93 | 5 |
| S2 | $20Ba–10TiO_2–70P_2O_5$ | 3.04 | 10 |
| S3 | $20Ba–15TiO_2–65P_2O_5$ | 3.18 | 15 |
| S4 | $20Ba–20TiO_2–60P_2O_5$ | 3.33 | 20 |

### 2.2. Calculation of the exposure build-up factor

The EBF values were calculated using the Phy-X/PSD online platform [9]. The platform applies the geometric-progression (G-P) fitting method with the ANSI/ANS-6.4.3 reference coefficients [10,11]. The equivalent atomic number (Zeq) is used to select/interpolate the G-P fitting coefficients for each glass and photon energy.

Calculations were performed at the 25 photon energies available in the selected Phy-X/PSD calculation grid and at penetration depths between 0.5 and 40 mfp. For comparison and graphical presentation, the EBF response is discussed at 1, 5, 10 and 20 mfp. The calculations are theoretical; no experimental EBF measurements for these exact compositions were available in the source manuscript.

## 3. Results and discussion

### 3.1. Energy dependence of EBF

The EBF exhibits a clear dependence on incident photon energy (Fig. 1). At energies below approximately 0.03 MeV, the values remain close to unity, indicating that the contribution of scattered photons to exposure is relatively small. With increasing photon energy, the EBF rises and forms a broad maximum in the approximate range of 0.4–0.8 MeV. This behaviour is associated with the increased contribution of Compton-scattered photons in this energy region. At higher energies, the EBF decreases as the photon interaction regime changes and the relative contribution of scattering to the exposure is reduced.

### 3.2. Effect of penetration depth

Penetration depth has a pronounced effect on EBF. As the depth increases from 1 to 20 mfp, the probability that photons undergo one or more scattering events before reaching the point of interest increases. Consequently, the EBF maxima become substantially larger. For TiO-1, the reported EBF values at the broad maximum are approximately 1.85, 6.18, 13.8 and 35.4 at 1, 5, 10 and 20 mfp,

respectively. This increase demonstrates that the scattered-photon contribution cannot be neglected in the evaluation of sufficiently thick glass shields.

### 3.3. Effect of $TiO_2$ content

The four compositions show similar overall energy-dependent trends, but a modest composition dependence is evident. Between 0.1 and 3 MeV, the $TiO_2$ -rich glass (TiO-4) generally exhibits a slightly lower EBF than the $TiO_2$ -poor glass (TiO-1), with the difference reaching approximately 8% at the largest penetration depths considered. The higher equivalent atomic number associated with the $TiO_2$ -rich composition contributes to this reduction in the build-up response. When expressed in mfp, however, the EBF differences among the four glasses remain relatively small, indicating that their build-up behaviour is broadly similar.

A secondary feature is observed immediately above the barium K-absorption edge, approximately within 0.04–0.08 MeV. This feature is more pronounced for TiO-4 at larger penetration depths and is associated with the rapid energy dependence of the equivalent atomic number around the absorption edge. G-P estimates in this narrow energy interval should therefore be interpreted with caution.

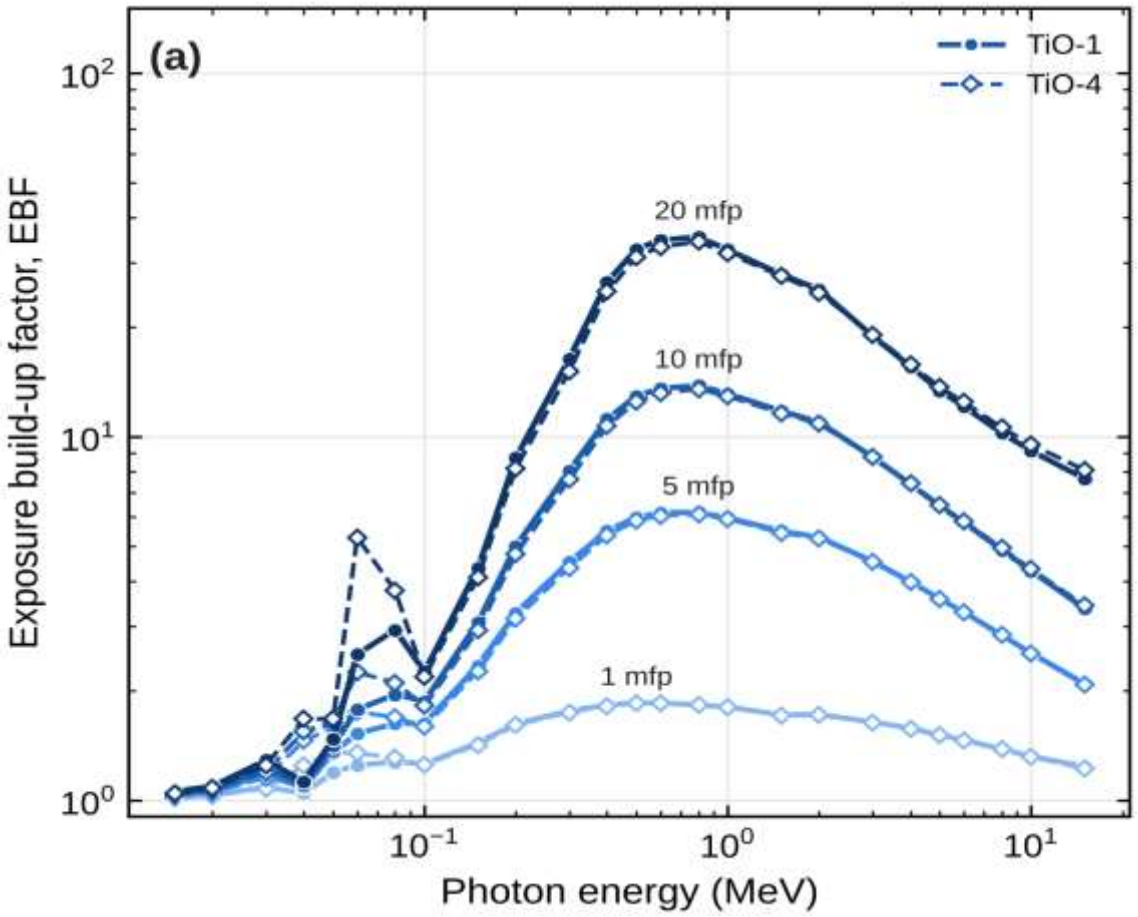


***Figure 1.*** *Exposure build-up factor (EBF) of TiO-1 and TiO-4 as a function of photon energy at penetration depths of 1, 5, 10 and 20 mean free paths.*

## 4. Limitations and outlook

The present results are based on calculations performed with Phy-X/PSD and the G-P fitting method; they are not experimental measurements. The accuracy of the calculated EBF values is therefore subject to the assumptions and applicability of the reference coefficients and interpolation procedure. In particular, the secondary feature near the Ba K-absorption edge should be treated cautiously. In addition, the calculations represent an idealised homogeneous shielding medium and do not explicitly account for finite-shield geometry, interfaces or material inhomogeneity. Future work should include experimental

characterisation of the glasses and independent radiation-transport simulations to validate the predicted EBF trends.

## 5. Conclusions

The exposure build-up factors of four Ba–$TiO_2$ –$P_2$ $O_5$ glasses were evaluated as functions of photon energy and penetration depth as given in the previous literatüre[12-19]. The principal conclusions are:

- The EBF remains close to unity at low photon energies, reaches a broad maximum in the 0.4–0.8 MeV region and decreases at higher energies.
- The EBF increases strongly with penetration depth. For TiO-1, representative maximum values are 1.85, 6.18, 13.8 and 35.4 at 1, 5, 10 and 20 mfp, respectively.
- The $TiO_2$ -rich glass exhibits a modestly lower EBF than the $TiO_2$ -poor glass between 0.1 and 3 MeV; the difference is up to approximately 8% at penetration depths as large as 20 mfp.
- The four glasses have broadly similar EBF trends when penetration depth is expressed in mfp. Nevertheless, the energy- and depth-dependent build-up contribution should be included when these materials are considered for broad-beam gamma-ray shielding.

## Author Statements:

- **Ethical approval:** The conducted research is not related to either human or animal use.
- **Conflict of interest:** The authors declare that they have no known competing financial interests or personal relationships that could have appeared to influence the work reported in this paper
- **Acknowledgement:** The authors declare that they have nobody or no-company to acknowledge.
- **Author contributions:** The authors declare that they have equal right on this paper.
- **Funding information:** The authors declare that there is no funding to be acknowledged.
- **Data availability statement:** The data that support the findings of this study are available on request from the corresponding author. The data are not publicly available due to privacy or ethical restrictions.
- **Use of AI Tools:** The author(s) declare that no generative AI or AI-assisted technologies were used in the writing process of this manuscript

## References

[1] Knoll, G.F., 2010. Radiation Detection and Measurement, 4th ed. John Wiley & Sons, Hoboken, NJ.
[2] Shultis, J.K., Faw, R.E., 2000. Radiation Shielding. American Nuclear Society, La Grange Park, IL.
[3] Brow, R.K., 2000. Review: the structure of simple phosphate glasses. Journal of Non-Crystalline Solids 263–264, 1–28. https://doi.org/10.1016/S0022-3093(99)00620-1
[4] Hoppe, U., Walter, G., Kranold, R., Stachel, D., 2000. Structural specifics of phosphate glasses probed by diffraction methods: a review. Journal of Non-Crystalline Solids 263–264, 29–47. https://doi.org/10.1016/S0022-3093(99)00621-3
[5] Kiani, A., Hanna, J.V., King, S.P., Rees, G.J., Smith, M.E., Roohpour, N., et al., 2012. Structural characterization and physical properties of $P_2O_5$–CaO–$Na_2O$–$TiO_2$ glasses. Acta Biomaterialia 8, 333–340.
[6] Silva, A.M.B., Correia, R.N., Oliveira, J.M.M., Fernandes, M.H.V., 2010. Structural characterization of $TiO_2$–$P_2O_5$–CaO glasses by spectroscopy. Journal of the European Ceramic Society 30, 1253–1258.
[7] Girón Lange, E., Youngman, R.E., Aitken, B.G., et al., 2025. Titanium phosphate glasses: Beyond tetrahedral network structures. Journal of Chemical Physics 163 (24).
[8] Haily, E., Bih, L., El Bouari, A., Lahmar, A., El Marssi, M., Manoun, B., 2020. Structural, optical, and dielectric properties of the BaO–$TiO_2$–$P_2O_5$ glasses. Journal of the Australian Ceramic Society 56, 1467–1479. https://doi.org/10.1007/s41779-020-00473-1
[9] Şakar, E., Özpolat, Ö.F., Alım, B., Sayyed, M.I., Kurudirek, M., 2020. Phy-X/PSD: Development of a user friendly online software for calculation of parameters relevant to radiation shielding and dosimetry. Radiation Physics and Chemistry 166, 108496. https://doi.org/10.1016/j.radphyschem.2019.108496
[10] American Nuclear Society, 1991. Gamma-Ray Attenuation Coefficients and Buildup Factors for Engineering Materials. ANSI/ANS-6.4.3-1991. American Nuclear Society, La Grange Park, IL.
[11] Harima, Y., Sakamoto, Y., Tanaka, S., Kawai, M., 1986. Validity of the geometric-progression formula in approximating gamma-ray buildup factors. Nuclear Science and Engineering 94, 24–35.
[12]Ghania BOUHILA, Fatima BENRACHI, & Mourad RAMDHANE. (2016). Evaluation of Natural Radioactivity and Assessment of Radiation Hazard Indices in Some Sediment Samples from Streams of East

Algeria. *International Journal of Sustainable Science and Technology*, *1*(1). https://doi.org/10.22399/ijsusat.20

[13]SOYAL, H., & SARIHAN, M. (2025). Radiation Safety Awareness for Future Healthcare Workers: Educational and Legal Perspectives. *International Journal of Biological-Medical Science and Technology*, *3*(1). https://doi.org/10.22399/ijbimes.1

[14]Betul Cetin, & Betul Sezer. (2025). Comparison of the radiation shielding effect of travertine and gasconcrete. *International Journal of Natural-Applied Sciences and Engineering*, *3*(1). https://doi.org/10.22399/ijnasen.31

[15]Abdelmoneim Saleh, Monir, N., Touti, R., & Keshavarz, S. (2026). Radiation Dose Distribution and Effective Dose Estimation in Adult Female Head CT. *International Journal of Biological-Medical Science and Technology*, *4*(1), 5–8. https://doi.org/10.22399/ijbimes.25 (Original work published June 24, 2026)

[16]Sibel ÖZAVCI, & Betül ÇETİN. (2017). Experimental Investigation of Radiation Shielding Effect in Different Doped Slag Concrete. *International Journal of Sustainable Science and Technology*, *2*(1). https://doi.org/10.22399/ijsusat.23

[17]Demet Sarıyer. (2025). A FLUKA-Based Study on the Effect of Boron-Enhanced Concrete on Secondary Neutron Dose under Proton Beam Loss Scenarios. *International Journal of Natural-Applied Sciences and Engineering*, *3*(1). https://doi.org/10.22399/ijnasen.30

[18]Betul Cetin, Arzu Poyraz, & Melek Gul. (2026). Examination of the radiation absorption parameters of CuO coatings prepared at different ratios. *International Journal of Sustainable Science and Technology*, *4*(1). https://doi.org/10.22399/ijsusat.35

[19]Menşure Canpolat, & Halil Soyal. (2025). The Relationship Between Radiation Safety and Ergonomics in Healthcare Workers: Comprehensive Protection Approaches. *International Journal of Biological-Medical Science and Technology*, *3*(1). https://doi.org/10.22399/ijbimes.21